blood advances

American Society of Hematology
2021 L Street NW, Suite 900,
Washington, DC 20036
Phone: 202-776-0544 | Fax 202-776-0545
bloodadvances@hematology.org

Biased agonism of protease-activated receptor-1 regulates thrombo-inflammation in murine sickle cell disease

Tracking no: ADV-2023-011907R2

Nirupama Ramadas (University of North Carolina at Chapel Hill, United States) Kailyn Lowder (University of North Carolina at Chapel Hill, United States) Joshua Dutton (University of North Carolina at Chapel Hill, United States) Fatima Trebak (University of North Carolina at Chapel Hill, United States) Camille Faes (University of Lyon, University Claude Bernard Lyon 1, France) John Griffin (The Scripps Research Institute, United States) Rafal Pawlinski (University of North Carolina at Chapel Hill, United States) Laurent Mosnier (The Scripps Research Institute, United States) Erica Sparkenbaugh (UNC Chapel Hill, United States)

Abstract:
Sickle cell disease (SCD) is a hereditary hemoglobinopathy marked by hemolytic anemia and vaso-occlusive events (VOE). Chronic endothelial activation, inflammation, and coagulation activation contribute to vascular congestion, VOE, and end-organ damage. Coagulation proteases like thrombin and activated protein C (APC) modulate inflammation and endothelial dysfunction by activating protease-activated receptor 1 (PAR1), a G-protein coupled receptor. Thrombin cleaves PAR1 at Arg41, while APC cleaves PAR1 at Arg46, initiating either pro-inflammatory or cytoprotective signaling, respectively, a signaling conundrum known as biased agonism. Our prior research established the role of thrombin and PAR1 in vascular stasis in an SCD mouse model. However, the role of APC and APC-biased PAR1 signaling in thrombin generation, inflammation and endothelial activation in SCD remains unexplored. Inhibition of APC in SCD mice increased thrombin generation, inflammation, and endothelial activation during both steady state and TNFα challenge. To dissect the individual contributions of thrombin-PAR1 and APC-PAR1 signaling, we employed transgenic mice with point mutations at two PAR1 cleavage sites, ArgR41Gln (R41Q) imparting insensitivity to thrombin and Arg46Gln (R46Q) imparting insensitivity to APC. Sickle bone marrow chimeras expressing PAR1-R41Q exhibited reduced thrombo-inflammatory responses compared to PAR1-WT or PAR1-R46Q mice. These findings highlight the potential benefit of reducing thrombin-dependent PAR1 activation while preserving APC-PAR1 signaling in SCD thromboinflammation. These results also suggest that pharmacological strategies promoting biased PAR1 signaling could effectively mitigate vascular complications associated with SCD.-

Conflict of interest: No COI declared

COI notes:

Preprint server: No;

Author contributions and disclosures: Contribution: NR conducted the experiments, analyzed data, and wrote the manuscript with consultation with EMS and contribution from all the co-authors; KL, JD, FT. and CF conducted experiments; JHG provided reagents. LOM provided reagents and consulted on experiments. RP consulted on experiments. EMS designed the experiments, performed experiments, analyzed the data, wrote the manuscript, and supervised the project.

Non-author contributions and disclosures: No;

Agreement to Share Publication-Related Data and Data Sharing Statement: Data can be shared by emails to the corresponding author.

Clinical trial registration information (if any):

Biased agonism of protease-activated receptor-1 regulates thrombo-inflammation in murine sickle cell disease

Nirupama Ramadas[1], Kailyn Lowder[1], Joshua Dutton[1], Fatima Trebak[1], Camille Faes[1†], John H. Griffin[2], Rafal Pawlinski[1], Laurent O. Mosnier[2], Erica Sparkenbaugh[1]

1- Department of Medicine, Division of Hematology, Blood Research Center, University of North Carolina, Chapel Hill, NC
2- Department of Molecular Medicine, The Scripps Research Institute, La Jolla CA

† - Deceased May 25, 2020.

Corresponding Author –

Erica Sparkenbaugh, PhD
Assistant Professor
Department of Medicine, Blood Research Center
University of North Carolina at Chapel Hill
116 Manning Drive, 8114 Mary Ellen Jones Bldg
Chapel Hill, NC, 27599
erica_sparkenbaugh@med.unc.edu
919-962-99580

Data can be shared by emails to the corresponding author.

Total Words: 3830

Abstract: 232

Figures: 5 figures, 3 tables

References: 54

Keywords: sickle cell disease, protease activated receptor-1, PAR1, thrombin, activated protein C, vascular occlusion

KEY POINTS

1. APC inhibition exacerbates thrombin generation, inflammation and end-organ damage in a mouse model of sickle cell disease (SCD).
2. APC-PAR1-R46 biased agonism reduces inflammation, suggesting that targeting this pathway may mitigate vascular complications of SCD.

ABSTRACT

Sickle cell disease (SCD) is a hereditary hemoglobinopathy marked by hemolytic anemia and vaso-occlusive events (VOE). Chronic endothelial activation, inflammation, and coagulation activation contribute to vascular congestion, VOE, and end-organ damage. Coagulation proteases like thrombin and activated protein C (APC) modulate inflammation and endothelial dysfunction by activating protease-activated receptor 1 (PAR1), a G-protein coupled receptor. Thrombin cleaves PAR1 at Arg41, while APC cleaves PAR1 at Arg46, initiating either pro-inflammatory or cytoprotective signaling, respectively, a signaling conundrum known as biased agonism. Our prior research established the role of thrombin and PAR1 in vascular stasis in an SCD mouse model. However, the role of APC and APC-biased PAR1 signaling in thrombin generation, inflammation and endothelial activation in SCD remains unexplored. Inhibition of APC in SCD mice increased thrombin generation, inflammation, and endothelial activation during both steady state and TNFα challenge. To dissect the individual contributions of thrombin-PAR1 and APC-PAR1 signaling, we employed transgenic mice with point mutations at two PAR1 cleavage sites, ArgR41Gln (R41Q) imparting insensitivity to thrombin and Arg46Gln (R46Q) imparting insensitivity to APC. Sickle bone marrow chimeras expressing PAR1-R41Q exhibited reduced thrombo-inflammatory responses compared to PAR1-WT or PAR1-R46Q mice. These findings highlight the potential benefit of reducing thrombin-dependent PAR1 activation while preserving APC-PAR1 signaling in SCD thromboinflammation. These results also suggest that pharmacological strategies promoting biased PAR1 signaling could effectively mitigate vascular complications associated with SCD.

INTRODUCTION

Sickle Cell Disease (SCD) is the most common inherited hemoglobinopathy worldwide, caused by a single nucleotide mutation in the gene for beta (β)-globin (1). This mutation results in a glutamine to valine substitution in the β globin chain, forming sickle hemoglobin (HbS). Upon deoxygenation, HbS undergoes abnormal polymerization, leading to the sickling of red blood cells (RBC). Sickle RBCs are prone to hemolysis and adhesion to other cells (platelets, neutrophils and endothelial cells), resulting in hemolytic anemia and vascular stasis, respectively (1, 2). A hypercoagulable state and increased risk of venous thrombosis are key characteristics of SCD (3-5). Tissue factor (TF)-dependent activation of extrinsic coagulation cascade contributes to inflammation, end-organ damage, and mortality in mouse models of SCD (6-9). Although non-hematopoietic protease activated receptor 1 (PAR1) does not contribute to systemic inflammation in a mouse model of SCD at steady state (7), a follow-up study revealed that thrombin-dependent PAR1 signaling promotes vascular stasis in sickle mice through upregulation of von Willebrand Factor (VWF) and P-selectin (P-sel) on the endothelium (10).

PAR1 is the main thrombin receptor on human platelets, but not mouse platelets, and is also expressed on leukocytes and endothelial cells (11, 12). This G protein coupled receptor is activated by proteolytic cleavage of specific amino acids on the extracellular N-terminus, forming tethered ligands that induce signaling. Thrombin cleaves PAR1 at Arg41 (R41), which activates Gαq and Gα12/13 signaling to initiate inflammation, endothelial barrier permeability, adhesion, and cytotoxicity (13, 14). PAR1 is also cleaved by activated protein C (APC), although with lower affinity than thrombin (15). Zymogen protein C (PC) binds the endothelial protein C receptor (EPCR), which serves two purposes. One, it colocalizes PC to thrombomodulin for efficient activation of PC by thrombomodulin-bound thrombin to generate APC. Two, EPCR colocalizes with PAR1 in caveolin-1 positive lipid rafts (16) to facilitate APC-mediated cleavage of PAR1 at Arg46 (R46), activating β-arrestin-dependent signaling that is anti-inflammatory and cytoprotective (16-18). Upon dissociation from EPCR and binding to negatively charged phospholipid surfaces, APC is also an endogenous anticoagulant that inactivates FVa and FVIIIa (17). Interestingly, individuals with SCD and sickle cell mice have lower levels of PC and APC activity (19-23), which decrease further during vaso-occlusive events (VOE) and negatively correlate with markers of coagulation activation (22). APC has beneficial effects in mouse models of sepsis, stroke, and experimental autoimmune encephalitis (24, 25), however its role in SCD has not been characterized. Here we set out to determine the role of endogenous APC activity and biased PAR1 agonism in a mouse model of SCD.

METHODS

Mice

Humanized SCD (Townes) mice express human α globin and either human sickle β globin ($\beta^S\beta^S$, HbSS) or normal adult β globin (β^A/β^A, HbAA or wild type control), and were bred in-house from HbAS breeding pairs. Male and female HbSS and HbAA littermate controls, aged 3-4 months were used for these studies. R41Q (thrombin cleavage insensitive) and R46Q (APC cleavage insensitive) transgenic mice (26) were utilized to investigate biased agonism of PAR1 in SCD. Mice were housed and maintained on a 12 hour light/dark schedule with food and water *ad libitum*. All animal experiments were approved by the University of North Carolina Institutional Care and Use Committee.

Bone Marrow Transplantation

HbAA and HbSS mouse bone marrow was transplanted into PAR1-WT, PAR1-R41Q and PAR1-R46Q recipients as previously described (7). Briefly, recipient mice were placed on acidified (pH 2.6) water containing neomycin (0.1 mg/mL) and polymyxin B sulfate (0.01 mg/mL (Sigma Aldrich) for one week before and two weeks after transplantation. A total of 1300 Gγ was administered in two equal exposures 4 hours apart. Bone marrow nucleated cells were harvested from HbAA and HbSS mice and resuspended in RPMI-1640 with 0.5% BSA (Gibco). A total of 5 x 10^6 donor bone marrow cells were intravenously injected in recipient mice 1 hour after the last irradiation. Engraftment of donor cells was analyzed using hemoglobin electrophoresis and only mice expressing human HbAA or HbSS were used for experiments 4 months after transplantation.

Inhibition of Endogenous APC Activity

Mice were treated with control IgG or SPC-54 (10 mg/kg, IP) (27) 24 hours before sample collection.

Tumor Necrosis Factor Challenge

In some studies, mice were challenged with recombinant murine tumor necrosis factor α (TNFα) to mimic vaso-occlusive crisis. Mice receive TNFα (2 mg/kg, IP) and samples were collected 5 hours later.

Sample Collection

Mice were anesthetized with isoflurane (3% in 100% oxygen) and blood was drawn from the inferior vena cava into syringes containing sodium citrate (3.8%, final ratio 9:1). Total blood cell count and hematologic profile were determined with a veterinary CBC analyzer (HT5, Heska). Plasma was collected by centrifugation at 4,000 rpm for 15 minutes at room temperature and stored at -80□C for future analysis.

Analysis of proinflammatory cytokines

ELISAs were used to quantify plasma levels of thrombin-antithrombin complex (TAT: Siemans Healthcare Diagnostics), pro-inflammatory cytokines IL-6, IL-18 (R&D Systems) and high mobility group box1 (HMGB1, Tecan) and endothelial activation

markers soluble vascular cell adhesion molecule 1, soluble intracellular adhesion molecule, soluble P-selectin (sVCAM-1, sICAM and sP-sel, R&D Systems) and Von Willebrand Factor (Abcam).

Tissue histology

Lungs, kidneys and livers were harvested from the mice, fixed in 10% formalin, and embedded in paraffin. Livers were sectioned (5 μm) and stained with hematoxylin and eosin (H&E), and congestion and necrosis were evaluated in the entire liver section at 20x magnification by 3 blinded researchers (NR, KL, and ES) according to the following criteria. Congestion (0-4): 0 – no red blood cells (RBCs) in sinusoids; 1 – RBCs in <10% of sinusoids; 2 – RBCs in <25% of sinusoids; 3 – RBCs in <50% of sinusoids; 4 – RBCs in >50% of sinusoids, bridging between veins, and RBCs present in parenchymal tissue. Necrosis (0-4): 0 – no obvious necrosis; 1 – necrosis in <10% of hepatocytes in field; 2 – necrosis in <25% of hepatocytes in field; 3 – necrosis in <50% of hepatocytes in field; 4 – necrosis in >50% of hepatocytes, bridging between central veins. Liver sections were also stained with Prussian blue and total Prussian blue area was quantified with Image J. Kidney sections (5 μm) were stained with H&E and red cell congestion was scored on a scale of 0-4 in the glomeruli in 10 high powered fields by 2 blinded researchers (ES and NR). The lungs were inflated with 10% formalin prior to collection. Lung sections (5 μm) were stained with H&E or for neutrophils. Before staining for neutrophils, lung sections underwent antigen retrieval (10 mM citrate buffer pH 6) for 20 minutes at 95°C, and endogenous peroxidases, avidin, and biotin were blocked with hydrogen peroxide (3%) and avidin/biotin blocking kit (Vector Labs), respectively. Neutrophil staining was performed using rat anti-mouse neutrophil monoclonal antibody (1:1000, NIMP-R14; Abcam) and biotinylated anti-rat secondary antibody (Vector Labs). Staining was developed with Vectastain ABC kit and ImmPACT DAB peroxidase substrate (Vector Labs) and counterstained with hematoxylin (Dako). Neutrophils were quantified in 10 high powered fields (400x) as previously described (7).

Statistical analysis

Data are presented as a mean ± SEM. One- or Two-way ANOVA were performed, with Tukey's post-hoc test for multiple comparisons. For data that are not normally distributed, Kruskall-Wallis and Dunn's multiple comparisons test were used (Graphpad Prism V9).

RESULTS

Inhibition of endogenous APC exacerbates thrombo-inflammation in sickle mice at steady state.

To investigate the role of APC in SCD, HbAA and HbSS mice were treated with control IgG or SPC54, a monoclonal antibody which binds to both APC and protein C and blocks APC's amidolytic activity (27) (Figure 1A). Blood was collected 24 hours after antibody administration. APC inhibition increased thrombin-antithrombin (TAT) in HbAA

mice, and significantly enhanced the already elevated TAT levels in HbSS mice (Figure 1B). APC inhibition also exacerbated inflammation, measured by plasma levels of IL-6 and IL-18 in both HbAA and HbSS mice (Figure 1C-D). Although APC inhibition did not alter plasma levels of sVCAM1, sICAM or VWF in HbSS mice (Figure 1E-G), it did significantly increase plasma levels of sP-sel (Figure 1H). P-selectin is stored in Weibel-Palade bodies of the endothelium, as well as platelet α granules. To determine the cellular source of the increased sP-sel in SPC54 treated HbSS mice, plasma levels of platelet factor 4 (PF4) were measured. PF4 is stored in platelet α granules but is not present in endothelial cells. There were similar levels of PF4 in IgG-treated HbAA and HbSS mice; SPC54 modestly reduced levels of PF4 in both HbAA and HbSS mice, but these were not significant (Figure 1J). This supports the conclusion that the elevation in sP-sel following SPC54 treatment indeed originates from endothelial cells. Moreover, SPC54 significantly reduced circulating platelet counts in HbAA and HbSS mice compared to IgG-treated controls (Table 1), likely due to vascular congestion in the organs. In contrast, SPC54 modestly increased circulating RBC parameters, neutrophils, and neutrophil: lymphocyte ratios in HbSS mice (Table 1), indicating that APC inhibition enhances acute inflammatory responses.

The effects of APC inhibition on organ damage were also evaluated. Histologic evaluation of the livers of SPC54-treated HbSS mice revealed enhanced vascular and sinusoidal congestion of RBCs and the presence of iron-laden macrophages (Figure 2A-B). APC inhibition did not increase hepatic necrosis (Figure 2C) or plasma levels of alanine aminotransferase (Figure 2D) in HbSS mice. Prussian blue staining confirms the presence of iron in the liver tissue of HbSS mice (Figure 2A), and quantification of total Prussian blue area showed that SPC-54 did not alter this (Figure 2E). These data suggesting that acute vascular congestion and thrombin generation do not exacerbate chronic hepatocyte damage. Lungs were stained for neutrophils (Figure 2F), which were counted in the alveolar spaces and walls. APC inhibition significantly increased the number of neutrophils in the lungs of HbSS mice (Figure 2G), consistent with the notion that inhibition of APC increases acute inflammatory responses. Kidney sections of both HbSS/IgG and HbSS/SPC54 showed congestion of sickled RBCs in glomeruli (Figure S1A-B). APC inhibition significantly increased glomerular congestion compared to IgG-treated HbSS mice (Figure S1C-D).

Inhibition of endogenous APC generation exacerbates thrombo-inflammation in sickle mice during TNFα challenge.

TNFα administration is a well-characterized model of acute inflammation that induces formation of multicellular aggregates, vascular stasis, and presence of thrombi in organs in HbSS mice (28-31). TNFα challenge exacerbates thrombin generation and inflammation in HbSS mice (31). To determine the role of APC in TNFα challenge, HbSS mice were treated with IgG or SPC54 19 hours before TNFα (2 mg/kg, IP) or saline (as steady-state) administration and samples were collected 5 hours later (Figure 3A). APC inhibition dramatically increased thrombin generation in TNFα-challenged

HbSS mice (Figure 3B). There was a similar pattern in the plasma levels of IL-6 (Figure 3C), and a trend to increased plasma levels of IL-18 in SS mice treated with TNFα (Figure 3D). In contrast, plasma levels of sVCAM, sICAM and VWF in HbSS mice were not significantly altered by TNFα challenge, with or without SPC-54 (Figure 3E-G), yet the endothelial activation marker sP-sel was increased (Figure 3H). This indicates that blocking endogenous APC generation enhances TAT, IL-6, IL-18, and sPsel in SCD mice after TNFα challenge.

Role of endogenous thrombin- and APC-biased agonism of PAR1

Since SPC54 blocks all APC activities, it was not possible to determine whether the anticoagulant or signaling properties of APC contribute to thrombin generation and inflammation in HbSS mice. To address this, bone marrow from HbSS mice (SS^{BM}) was transplanted into PAR1 modified mice with point mutations in the respective thrombin and APC cleavage sites that make them insensitive to either thrombin (R41Q) or APC (R46Q) cleavage (26). This approach yielded SS^{BM}/WT, SS^{BM}/R41Q and SS^{BM}/R46Q mice (Figure 4A). Neither the R41Q nor R46Q mutation affected anemia or neutrophilia in SS mice (Table 3).

At steady state, there was no difference in TAT in SS^{BM}/R41Q or SS^{BM}/R46Q mice compared to SS^{BM}/WT mice. TNFα challenge enhanced TAT levels in SS^{BM}/WT mice, which was significantly attenuated in SS^{BM}/R41Q mice. Although TAT levels were higher in SS^{BM}/R46Q mice compared to SS^{BM}/R41Q, they were not elevated compared to SS^{BM}/WT mice (Figure 4B), indicating that thrombin-mediated PAR1 activation contributes to enhanced thrombin generation. Similarly, the inflammatory cytokine IL-6 was not affected by the PAR1 point mutations at steady state. In contrast, the elevated levels of IL-6 observed in TNFα-treated SS^{BM}/WT mice were attenuated in SS^{BM}/R41Q mice, and further exacerbated in SS^{BM}/R46Q mice (Figure 4C). Plasma levels of HMGB1 were elevated by TNFα challenge and were attenuated in SS^{BM}/R41Q compared to SS^{BM}/WT or SS^{BM}/R46Q mice (Figure 4D). The inflammatory cytokine IL-18 was significantly upregulated in SS^{BM}/R46Q mice at steady state, yet was not further increased by TNFα challenge (Figure 4E). These results suggest that thrombin-mediated PAR1 cleavage fuels inflammation whereas APC-mediated PAR1 activation attenuates inflammation.

The endothelial activation markers sVCAM and VWF were not altered in SS^{BM}/R41Q and SS^{BM}/R46Q mice compared to SS^{BM}/WT controls at steady state or during TNF challenge (Figure 4F and 4G). In contrast, TNFα challenge increased the levels of sP-sel and sICAM in all SS mice (Figure 4G and 4I), however these markers were not different from SS^{BM}/WT in either SS^{BM}/R41Q or SS^{BM}/R46Q mice. Neither PAR1 expression nor TNFα challenge affected plasma levels of PF4 (Figure 4I), suggesting that endothelial cells, rather than platelets, are the source of sP-sel after TNFα treatment.

Histological analysis of the livers for vascular congestion revealed vascular congestion of sickled RBCs, the presence of iron-laden macrophages, and necrosis in the livers of all SS^{BM} mice (Figure 5A). When the pathology was scored, we found significantly more RBC-mediated congestion in SS^{BM}/R46Q mice than SS^{BM}/WT or SS^{BM}/R41Q mice at steady state (Figure 5B). Interestingly, TNFα challenge increased vascular congestion in SS^{BM}/WT and SS^{BM}/R41Q mice compared to their saline-treated counterparts, whereas TNFα did not further increase vascular congestion in SS^{BM}/R46Q mice (Figure 5B). Neither TNFα challenge nor PAR1 cleavage site mutations had any significant effect on hepatic necrosis scores (Figure 5C). Prussian blue staining revealed the presence of iron in the liver tissue (Figure 5A), yet quantification of Prussian blue revealed no differences between the PAR1 genotypes. Evaluation of lung pathology revealed the presence of sickled RBCs in the interstitial tissues of all SS^{BM} mice, regardless of PAR1 expression or TNF challenge (Figure S2). Kidney histopathology revealed increased congestion of sickled RBCs in the SS^{BM}/WT and SS^{BM}/R46Q mice compared to AA^{BM}/WT (Figure S3). Interstitial and glomerular congestion were quantified but there were no differences between $SS^{BM/}$WT, SS^{BM}/R41Q and SS^{BM}/R46Q mice (Figure S3B-C)

DISCUSSION

A recent global analysis found that SCD affects nearly 8 million people worldwide, with over 500 000 new births in 2021 (32). It is the twelfth leading cause of death for children under 5, and total mortality has increased by 20% since 2000 (32). In spite of this, there are only four FDA-approved treatment options for patients: hydroxyurea, crizanlizumab, L-glutamine, and voxelotor (1). These therapies only modestly limit the severity and frequency of hemolytic and vascular complications (33-35). Coagulation activation and thrombotic complications are a hallmark of SCD, and an estimated 11-27% of patients experience venous thrombosis (5). In addition to thrombotic complications, SCD is characterized by endothelial dysfunction and adhesion, which contributes to vascular stasis and ultimately vaso-occlusive crisis (1, 2). APC is uniquely situated in both of these pathways, due to its role as an anticoagulant and in maintaining endothelial homeostasis through biased activation of PAR1 (36). However, the role of APC has not been extensively investigated in SCD.

In this study, the role of the endogenous APC system was assessed in HbSS mice by inhibiting APC generation using antibody SPC54. Notably, APC inhibition significantly increased thrombin generation, systemic inflammation, and the release of soluble P-selectin in HbSS mice under steady-state conditions. A marked rise in vascular congestion in the liver, heightened neutrophil accumulation in the lungs, and worsened red blood cell congestion in the kidneys were observed. These findings suggest that inhibition of APC generation enhances thrombin generation, leading to the hypothesis that this process triggers PAR1-dependent pro-inflammatory signaling and release of P-sel from Weibel-Palade bodies at steady state and after TNFα challenge. Accordingly, a potential protective role of endogenous APC in SCD by limiting thrombin generation is

surmised. Importantly, individuals with SCD have decreased PC and APC activity levels compared to healthy controls, with further reductions during VOE (23, 37-40). Furthermore, the decreased APC activity correlates with an increased risk of stroke and thrombosis (21, 40).

Since APC has both anticoagulant and cytoprotective signaling functions through activation of PAR1, biased agonism of PAR1 by APC in HbSS mice was also evaluated. We previously showed that PAR1 deficiency on non-hematopoietic cells had no effect on thrombin generation or plasma levels of IL-6 at steady state in HbSS mice (7). One interpretation of these results is that PAR1 does not play a role in inflammation and endothelial activation in steady state disease. Another possibility is that PAR1 deletion removes both detrimental thrombin/PAR1 signaling, as well as beneficial APC/PAR1 signaling (18). To address this limitation of gene knockout studies, Sinha et al. generated mice with point mutations in PAR1 that are selectively activated by either thrombin or APC to investigate the individual contributions of these two pathways (26). Consistent with previous results (7), neither SS^{BM}/R41Q nor SS^{BM}/R46Q mice exhibited differences in thrombin generation, endothelial activation, or systemic inflammation compared to the $SS^{BM}/PAR1^{WT}$ counterparts at steady state. However, hepatic vascular congestion was significantly increased in the SS^{BM}/R46Q mice at steady state compared to SS^{BM}/WT and SS^{BM}/R41Q mice. This observation suggests a protective role for endogenous APC/PAR1 signaling against vascular congestion. Since we previously showed that PAR1 contributes to heme-induced vascular stasis in HbSS mice (10), future studies will determine the individual roles of thrombin- and APC-biased agonism on this complication. It will also be interesting to determine if long-term biased agonism of either the thrombin/PAR1 or APC/PAR1 pathways contributes to end-organ damage and mortality.

Following TNFα challenge, SS^{BM}/R41Q mice exhibited lower TAT levels than both SS^{BM}/WT and SS^{BM}/R46Q mice, suggesting that thrombin/PAR1 signaling plays a role in the heightened thrombin generation in this model of VOE. We hypothesize that this is an indirect effect, wherein canonical thrombin/PAR1 signaling increases endothelial permeability, thus exposing perivascular tissue factor (TF) to the blood to initiate more thrombin generation and resulting in elevated circulating TAT levels. Indeed, our previous work demonstrated that perivascular TF plays a role in thrombin generation in HbSS mice (8). Additionally, these findings suggest that thrombin/PAR1 signaling contributes to endothelial activation, consistent with our previous finding that inhibiting PAR1 with vorapaxar or deficiency in non-hematopoietic PAR1 reduced P-sel expression on the endothelial surface.

Remarkably, SS^{BM}/R41Q mice demonstrated protection against TNFα-enhanced IL-6, IL-18, and HMGB1 levels, while sickle mice expressing SS^{BM}/R46Q exhibited elevated IL-6 levels when compared to both SS^{BM}/WT and SS^{BM}/R41Q mice. These findings strongly suggest that thrombin-PAR1-R41 signaling increases inflammation and APC-PAR1-R46 signaling blunts inflammation. Thus, biased agonism of PAR1 differentially

regulates inflammation in SCD during a VOE-like challenge. These data are consistent with the worsened IL-6 and IL-18 levels observed with SPC-54-mediated APC inhibition. Inflammatory cytokines like IL-6 and IL-18 can be secreted from activated endothelial cells and leukocytes. In the present studies, we can only investigate the role of non-hematopoietic PAR1 signaling due to the nature of the bone marrow transplantation approach. Although the primary source of these cytokines in HbSS mice cannot be identified, our data suggest that endothelial cells contribute to elevated cytokine levels during TNFα challenge.

This study revealed notable differences in the regulation of sVCAM and sP-sel, two markers of endothelial activation, in response to APC inhibition and biased PAR1 signaling. Plasma sVCAM-1 levels were unaffected by APC inhibition or either PAR1 point mutation. In the context of SCD, elevated sVCAM-1 levels are primarily attributed to increased endothelial expression and proteolytic release (41). Our data suggest that this process is not influenced by PAR1 signaling. In contrast, P-sel is stored in Weibel-Palade bodies with VWF. In SCD, thrombin-PAR1-R41 signaling is known to release Weibel-Palade bodies from endothelial cells to increase endothelial surface and plasma levels of VWF and P-sel (10, 42, 43). Indeed, APC inhibition with SPC-54 significantly raised sP-sel levels, at steady state and during TNFα challenge in SS mice. To discern the source of sP-sel, considering its potential release from platelet α granules after thrombin activation of PAR4 in mice (44), we examined plasma levels of PF4, stored in α granules but not endothelial cells. No increase in PF4 was observed in HbSS mice compared to HbAA, and APC inhibition had no impact on PF4 levels, suggesting that in this context, sP-sel release originated from endothelial cells rather than platelets.

However, the approach of inhibiting APC alone does not elucidate if the increase in sP-sel is a result of canonical thrombin-PAR1-R41 signaling (due to increased thrombin generation), or inhibition of protective APC-PAR1-R46 signaling. To address that, we evaluated sP-sel levels in our SS^{BM} mice with PAR1 point mutations. Interestingly, sP-sel levels were not different from SS^{BM}/WT mice in either SS^{BM}/R41Q and SS^{BM}/R46Q mice at steady state or TNFα challenge, suggesting that PAR1 signaling does not contribute to release of sP-sel in this model. One possible explanation is that PAR1 signaling primarily influences P-selectin expression on the surface but not release of sP-sel into the circulation. Weibel-Palade body release is also stimulated by other agonists such as vascular endothelial growth factor (45), histamine (46), vasopressin, and sphingosine 1 phosphate (47), suggesting that these effectors may play a role in this pathway in this context.

Circulating levels of VWF were modestly increased in HbSS after TNFα challenge, consistent with previous reports (30). Interestingly, unlike sP-sel, there were no discernable differences in VWF levels between SS^{BM}/WT, SS^{BM}/R41Q and SS^{BM}/R46Q mice at steady state or after TNFα challenge, suggesting that biased agonism of PAR1 does not impact VWF release into the circulation. It is possible that although the assay did not detect differences in total VWF among the groups, differences in the size

distribution of the VWF multimers may exist. ADAMTS13, a metalloprotease controlling VWF cleavage and ultra-large VWF multimer degradation, exhibits decreased activity in SCD (30). APC has been demonstrated to increase ADAMTS13 mRNA in endothelial cells treated with plasma from sepsis patients. It is possible that APC-PAR1-R46 biased agonism may influence ADAMTS13 activity and thus VWF multimer size, yet this remains to be tested.

In conclusion, our study demonstrates that APC inhibition exacerbates thrombin generation and inflammation both under steady state conditions and during acute TNFα challenge that models VOE. Our findings offer insight into the intricate interplay between canonical thrombin-PAR1-R41 signaling, inflammation and endothelial activation in sickle mice, while underscoring the benefits of APC-PAR1-R46 signaling in reducing inflammation. These results highlight a multifaceted role for PAR1 signaling and APC in SCD. Since APC can limit thrombin generation and promote PAR1-dependent beneficial biased signaling following R46 cleavage, the potential therapeutic implications of leveraging this biased role of PAR1 to mitigate vascular complications associated with SCD is promising and merits further studies. Indeed, these results extend beyond SCD, suggesting a broader relevance to inflammatory conditions in which PAR1 has been implicated, such as cardiovascular disease (48-51), stroke (52), viral infections (53), sepsis (26) and colitis (54). It will be interesting to determine if PAR1 modulators such as parmodulins or pepducins will be beneficial in this setting.

ACKNOWLEDGEMENTS

Thank you to Robert Lee and David Paul for helpful conversations about our results. EMS is supported by R01 HL155193 and an ASH Scholar Award. LOM is supported by R01HL148096, R01 HL142975, and R01HL104165. RP is supported by R01 HL157441. JHG is supported by R01 HL142975.

CONFLICT OF INTEREST DISCLOSURE

EMS and RP are supported by research funding from CSL Behring for an un-related project.

AUTHORSHIP CONTRIBUTIONS

Contribution: NR conducted the experiments, analyzed data, and wrote the manuscript with consultation with EMS and contribution from all the co-authors. KL, JD, FT and CF conducted experiments. JHG provided reagents. LOM provided reagents and consulted on experiments. RP consulted on experiments. EMS designed the experiments, performed experiments, analyzed the data, wrote the manuscript, and supervised the project.

FIGURE LEGENDS:

Figure 1: Inhibition of endogenous APC by SPC-54 exacerbates the thrombo-inflammation at steady state in HbSS mice. Four month old HbAA (gray) and HbSS (blue) mice were treated with 10 mg/kg (i.p.) IgG (solid bars) or SPC54 (white hashed bars) and samples were collected 24 hours later (A). Plasma levels of (B) TAT, (C) IL-6, (D) IL-18, (E) sVCAM, (F) sICAM, (G) VWF, (H) sP-sel, and (I) Platelet factor 4 (PF4). Data are represented by mean ± SEM of n=5-6 mice per group, and analyzed by Two Way ANOVA and Tukey's post-hoc test. Asterisks directly above the bars indicate statistical significance of SS mice to AA mice in same treatment group. Asterisks over brackets indicate difference from IgG-treated mice. *p< 0.05, ** p< 0.01, ***p< 0.001 and ****p< 0.0001. SS, Sickle mice; AA, Controls.

Figure 2: APC inhibition exacerbates hepatic congestion and lung neutrophil accumulation. (A) Representative images of liver sections from HbSS mice treated with IgG or SPC-54 stained with H&E (top panels) and Prussian Blue (bottom panels). Black arrow indicates sinusoidal congestion, green arrow indicates iron-laden macrophages. Quantification of (B) liver congestion and (C) liver necrosis by three blinded observers. (D) Plasma levels of alanine aminotransferase (ALT). (E) Quantification of Prussian blue stain per total area. (F) Representative images of lung sections stained for neutrophils (brown). Scale bar represents 50 µm, red asterisk (*) denotes neutrophils. (G) Quantification of neutrophils averaged over 10 high powered (40x) fields. Data are represented by mean ± SEM of n=5-6 mice per group, and analyzed by Two Way ANOVA and Tukey's post-hoc test. Asterisks directly above the bars indicate statistical significance of SS mice to AA mice in same treatment group. Asterisks over brackets indicate difference from IgG-treated mice. *p< 0.05, ** p< 0.01, ***p< 0.001 and ****p< 0.0001. SS, Sickle mice; AA, Controls.

Figure 3: Inhibition of endogenous APC by SPC54 exacerbates thromboinflammation in HbSS mice after TNFα challenge. Male and female HbSS mice were treated with IgG or SPC-54 (10 mg/kg, IP) 19 hours before SAL or TNFα (2 µg/kg, IP) and plasma was collected 5 hours later (A). Plasma levels of (B) TAT, (C) IL-6, (D) IL-18, (E) sVCAM1, (F) sICAM, (G) VWF, and (H) sP-sel. Data represent mean ± SEM mean of n=5-10 mice per group. Asterisks above brackets indicate statistical significance by One way ANOVA with Kruskal-Wallis post-test. *p<0.05, ***p<0.001, ****p<0.0001.

Figure 4: Effect of PAR1 biased agonism on biomarkers of coagulation and inflammation. SS bone marrow was transplanted into lethally irradiated WT (gray), R41Q (red) and R46Q (purple) mice. Four months later, mice were treated with SAL (steady state, solid bars) or TNFα (2 mg/kg, IP) (black hashed bars) and plasma was collected after 5 hours (A). Plasma levels of (B) TAT, (C) IL-6, (D) HMGB1, (E) IL-18, (F) sVCAM-1, (G) sICAM, (H) VWF, (I) sP-sel and (J) PF4. Data represent mean ± SEM. N=6-8 mice (SAL, steady state) and n=15-17 mice per group for TNFα challenge.

Asterisks above bar represent statistical significance versus SAL-treated mice of same genotype by Two Way ANOVA and Tukey's post-hoc test. Asterisks above brackets indicate comparison. *p<0.05, **p<0.01, ***p<0.001, and ****p<0.0001.

Figure 5: Hepatic congestion is enhanced in SS^{BM}/R46Q mice. Livers were collected and stained with H&E; representative images of livers from SS^{BM}/WT, SS^{BM}/R41Q, and SS^{BM}/R46Q mice during steady state (SAL) and TNFα challenge; scale bar represents 50 μm (A). Three blinded observers (scored (B) congestion and (C) necrosis. Data represent mean ± SEM. Black arrow denotes sinusoidal congestion and green arrow denotes iron-laden macrophages. There were n=6-8 mice (SAL, steady state) and n=15-17 mice (TNFα challenge) per group. Asterisks above bar represent statistical significance versus SAL-treated mice of same genotype by Two Way ANOVA and Tukey's post-hoc test. Asterisks above brackets indicate comparison. *p<0.05.

TABLES

Parameter	AA/IgG (n=5)	AA/SPC-54 (n=5)	SS/IgG (n=5)	SS/SPC-54 (n=6)
RBC (10^6/μL)	9.33 ± 0.19	7.09 ± 0.85*	5.05±0.32****	6.40 ± 0.06*
Hgb (g/dL)	9.56 ± 0.34	7.5 ± 0.93*	6.08 ± 0.41***	8.53 ± 0.24##
Hematocrit (%)	31.8 ± 0.88	24.1 ± 3.02*	22.92 ± 1.69**	31.85 ± 0.72##
PMN:Lymph	0.15 ± 0.14	1.63 ± 0.34***	0.28 ± 0.05	1.29 ± 0.17##
WBC (10^3/μL)	8.07 ± 0.74	9.21 ± 0.78	29.63 ± 6.1**	23.21 ± 2.1*
PMN (10^3/μL)	0.98 ± 0.05	5.45 ± 0.76*	6.87 ± 2.19***	12.54±1.11****##
Lymphocytes (10^3/μL)	6.79 ± 0.70	3.49 ± 0.37	22.01 ± 3.9***	10.21 ± 1.19##
Monocytes (10^3/μL)	0.21 ± 0.03	0.24 ± 0.04	0.57 ± 0.12*	0.35 ± 0.07
Platelet (10^3/μL)	895 ± 23.7	213.0 ± 16.3***	814.0 ± 63.7	258 ± 18.0###

Table 1. Complete blood counts from AA and SS mice treated with IgG or SPC-54. *p<0.05, *p<0.01, *p<0.001, *p<0.0001 vs AA/IgG; ##p<0.01 vs SS/IgG. RBC – red blood cell; Hgb – hemoglobin; WBC – total white blood cell count; PMN – polymorphonuclear lymphocyte (neutrophil).

Variable	AA	SS		
	IgG (n=3)	IgG (n=5)	IgG / TNF (n=10)	SPC-54 / TNF (n=10)
RBC (10^6/μL)	9.50 ± 0.072	6.57 ± 0.35*	5.77 ± 0.15**	5.62 ± 0.21**
Hematocrit (%)	34.2 ± 2.6	34.2 ± 2.55	30.56 ± 2.14	25.55 ± 1.55$
PMN:Lymph	0.21 ± 0.04	0.17 ± 0.05	0.53 ± 0.18$	1.07 ± 0.12$
WBC (10^3/μL)	10.75 ± 1.28	31.3 ± 4.42*	25.8 ± 3.59	28.21 ± 6.69
PMN (10^3/μL)	1. 57 ± 0.25	12.37 ± 2.34**	28.77 ± 4.95$$	49.32±2.36**$
Lymphocyte 10^3/μL)	75.85 ± 2.75	77.13 ± 6.52	66.23 ± 5.88	47.38 ± 2.55
Monocyte (10^3/μL)	4.8 ± 1.55	3.43 ± 1.68	3.8 ± 0.74	2.42 ± 0.25
Platelet (10^3/μL)	950 ± 82.5	919 ± 245	903 ± 320	268 ± 111.4**$$

Table 2. Hematologic parameters from AA and SS mice after SPC-54 and TNFα treatment. * indicate statistical difference compared to AA IgG (*p< 0.05, **p< 0.01 and ***p< 0.005). $ indicate statistical difference compared to SS IgG ($^{\$}p$ < 0.05, $^{\$\$}p$ < 0.01)

Variable	SS at steady state			SS after TNFα challenge		
	WT	**PAR1^{41Q}**	**PAR1^{46Q}**	**WT**	**PAR1^{41Q}**	**PAR1^{46Q}**
RBC (10^6/μL)	5.49 ± 0.08	5.65 ± 0.15	5.65 ± 0.17	4.98 ± 0.21	4.95 ± 0.15	5.13 ± 0.17
Hematocrit (%)	26.46 ± 0.44	27.32 ± 0.68	27.24 ± 0.74	24.1 ± 0.77	23.69 ± 0.69	24.03 ± 0.65
PMN:Lymph	0.21 ± 0.002	0.21 ± 0.002	0.21 ± 0.01	0.21 ± 0.01	0.21 ± 0.004	0.22 ± 0.003
WBC (10^3/μL)	31.34 ± 1.71	30.81 ± 1.62	30.16 ± 1.67	14.59 ± 1.38	15.31 ± 1.14	13.65 ± 1.44
Neutrophil (10^3/μL)	3.73 ± 0.41	3.6 ± 0.29	4.78 ± 0.47	3.23 ± 0.29	3.36 ± 0.16	3.41 ± 0.43
Lymphocyte 10^3/μL)	17.74 ± 3.08	21.42 ± 2.78	20.41 ± 2.85	9.05 ± 1.33	10.72 ± 1.37	8.99 ± 1.3
Monocyte (10^3/μL)	0.6 ± 0.07	0.72 ± 0.15	1.06 ± 0.23	0.14 ± 0.03	0.19 ± 0.04	0.21 ± 0.07
Platelet (10^3/μL)	748 ± 43.9	721 ± 33.7	618 ± 47.6	589 ± 62.5	598.9 ± 45.9	486.8 ± 35.6

Table 3. Hematologic parameters from SS^{WT}, PAR1^{R41Q} and PAR1^{46Q} mice with bone marrow transplanted from SS mice Asterisks indicate statistical difference compared to SS WT within the same condition (*p< 0.05, **p< 0.01 and ***p< 0.005).

LITERATURE CITED

1. Kavanagh PL, Fasipe TA, & Wun T (2022) Sickle Cell Disease: A Review. *JAMA : the journal of the American Medical Association* 328(1):57-68.
2. Kato GJ*, et al.* (2018) Sickle cell disease. *Nat Rev Dis Primers* 4:18010.
3. Brunson A, Keegan T, Mahajan A, White R, & Wun T (2019) High incidence of venous thromboembolism recurrence in patients with sickle cell disease. *American journal of hematology* 94(8):862-870.
4. Brunson A*, et al.* (2017) Increased incidence of VTE in sickle cell disease patients: risk factors, recurrence and impact on mortality. *British journal of haematology* 178(2):319-326.
5. Lizarralde-Iragorri MA & Shet AS (2020) Sickle Cell Disease: A Paradigm for Venous Thrombosis Pathophysiology. *Int J Mol Sci* 21(15):5279.
6. Sparkenbaugh EM*, et al.* (2016) Thrombin-independent contribution of tissue factor to inflammation and cardiac hypertrophy in a mouse model of sickle cell disease. *Blood* 127(10):1371-1373.
7. Sparkenbaugh EM*, et al.* (2014) Differential contribution of FXa and thrombin to vascular inflammation in a mouse model of sickle cell disease. *Blood* 123(11):1747-1756.
8. Chantrathammachart P*, et al.* (2012) Tissue factor promotes activation of coagulation and inflammation in a mouse model of sickle cell disease. *Blood* 120(3):636-646.
9. Arumugam PI*, et al.* (2015) Genetic diminution of circulating prothrombin ameliorates multiorgan pathologies in sickle cell disease mice. *Blood* 126(15):1844-1855.
10. Sparkenbaugh EM*, et al.* (2020) Thrombin activation of PAR-1 contributes to microvascular stasis in mouse models of sickle cell disease. *Blood* 135(20):1783-1787.
11. Vu TK, Wheaton VI, Hung DT, Charo I, & Coughlin SR (1991) Domains specifying thrombin-receptor interaction. *Nature* 353(6345):674-677.
12. Vu TK, Hung DT, Wheaton VI, & Coughlin SR (1991) Molecular cloning of a functional thrombin receptor reveals a novel proteolytic mechanism of receptor activation. *Cell* 64(6):1057-1068.
13. Posma JJ*, et al.* (2019) Roles of Coagulation Proteases and PARs (Protease-Activated Receptors) in Mouse Models of Inflammatory Diseases. *Arteriosclerosis, thrombosis, and vascular biology* 39(1):13-24.
14. Willis Fox O & Preston RJS (2020) Molecular basis of protease-activated receptor 1 signaling diversity. *Journal of thrombosis and haemostasis : JTH* 18(1):6-16.
15. Ludeman MJ*, et al.* (2005) PAR1 cleavage and signaling in response to activated protein C and thrombin. *The Journal of biological chemistry* 280(13):13122-13128.
16. Bae JS, Yang L, & Rezaie AR (2007) Receptors of the protein C activation and activated protein C signaling pathways are colocalized in lipid rafts of endothelial cells. *Proceedings of the National Academy of Sciences of the United States of America* 104(8):2867-2872.

17. Mosnier LO, Sinha RK, Burnier L, Bouwens EA, & Griffin JH (2012) Biased agonism of protease-activated receptor 1 by activated protein C caused by noncanonical cleavage at Arg46. *Blood* 120(26):5237-5246.
18. Griffin JH, Zlokovic BV, & Mosnier LO (2015) Activated protein C: biased for translation. *Blood* 125(19):2898-2907.
19. Francis RB, Jr. (1988) Protein S deficiency in sickle cell anemia. *The Journal of laboratory and clinical medicine* 111(5):571-576.
20. Marfaing-Koka A*, et al.* (1993) Decreased protein S activity in sickle cell disease. *Nouv Rev Fr Hematol (1978)* 35(4):425-430.
21. Tam DA (1997) Protein C and protein S activity in sickle cell disease and stroke. *J Child Neurol* 12(1):19-21.
22. Westerman MP*, et al.* (1999) Antiphospholipid antibodies, proteins C and S, and coagulation changes in sickle cell disease. *The Journal of laboratory and clinical medicine* 134(4):352-362.
23. Schnog JB*, et al.* (2004) Protein C and S and inflammation in sickle cell disease. *American journal of hematology* 76(1):26-32.
24. Zlokovic BV*, et al.* (2005) Functional recovery after embolic stroke in rodents by activated protein C. *Annals of neurology* 58(3):474-477.
25. Kant R, Halder SK, Fernandez JA, Griffin JH, & Milner R (2020) Activated Protein C Attenuates Experimental Autoimmune Encephalomyelitis Progression by Enhancing Vascular Integrity and Suppressing Microglial Activation. *Front Neurosci* 14:333.
26. Sinha RK*, et al.* (2018) PAR1 biased signaling is required for activated protein C in vivo benefits in sepsis and stroke. *Blood* 131(11):1163-1171.
27. Burnier L, Fernandez JA, & Griffin JH (2013) Antibody SPC-54 provides acute in vivo blockage of the murine protein C system. *Blood Cells Mol Dis* 50(4):252-258.
28. Hidalgo A*, et al.* (2009) Heterotypic interactions enabled by polarized neutrophil microdomains mediate thromboinflammatory injury. *Nature medicine* 15(4):384-391.
29. Chen G*, et al.* (2014) Heme-induced neutrophil extracellular traps contribute to the pathogenesis of sickle cell disease. *Blood* 123(24):3818-3827.
30. Shi H*, et al.* (2022) Endothelial VWF is critical for the pathogenesis of vaso-occlusive episode in a mouse model of sickle cell disease. *Proceedings of the National Academy of Sciences of the United States of America* 119(34):e2207592119.
31. Sparkenbaugh EM*, et al.* (2023) Factor XII contributes to thrombotic complications and vaso-occlusion in sickle cell disease. *Blood*.
32. Collaborators GBDSCD (2023) Global, regional, and national prevalence and mortality burden of sickle cell disease, 2000-2021: a systematic analysis from the Global Burden of Disease Study 2021. *Lancet Haematol*.
33. Niihara Y*, et al.* (2018) A Phase 3 Trial of l-Glutamine in Sickle Cell Disease. *The New England journal of medicine* 379(3):226-235.
34. Sethy S, Panda T, & Jena RK (2018) Beneficial Effect of Low Fixed Dose of Hydroxyurea in Vaso-occlusive Crisis and Transfusion Requirements in Adult

HbSS Patients: A Prospective Study in a Tertiary Care Center. *Indian J Hematol Blood Transfus* 34(2):294-298.
35. Ataga KI*, et al.* (2016) Crizanlizumab for the Prevention of Pain Crises in Sickle Cell Disease. *The New England journal of medicine*.
36. Rezaie AR (2010) Regulation of the protein C anticoagulant and antiinflammatory pathways. *Curr Med Chem* 17(19):2059-2069.
37. el-Hazmi MA, Warsy AS, & Bahakim H (1993) Blood proteins C and S in sickle cell disease. *Acta haematologica* 90(3):114-119.
38. Guo Y*, et al.* (2008) The Protein C Pathway in Human and Murine Sickle Cell Disease: Alterations in Protein C, Thrombomodulin (TM), and Endothelial Protein C Receptor (EPCR) at Baseline and during Acute Vaso-Occlusion. *Blood* 112(11):202-202.
39. Karayalcin G & Lanzkowsky P (1989) Plasma protein C levels in children with sickle cell disease. *Am J Pediatr Hematol Oncol* 11(3):320-323.
40. Khanduri U*, et al.* (1998) Reduced protein C levels--a contributory factor for stroke in sickle cell disease. *Thrombosis and haemostasis* 79(4):879-880.
41. Belcher JD*, et al.* (2003) Transgenic sickle mice have vascular inflammation. *Blood* 101(10):3953-3959.
42. Embury SH*, et al.* (2004) The contribution of endothelial cell P-selectin to the microvascular flow of mouse sickle erythrocytes in vivo. *Blood* 104(10):3378-3385.
43. Matsui NM*, et al.* (2001) P-selectin mediates the adhesion of sickle erythrocytes to the endothelium. *Blood* 98(6):1955-1962.
44. Hamilton JR, Cornelissen I, & Coughlin SR (2004) Impaired hemostasis and protection against thrombosis in protease-activated receptor 4-deficient mice is due to lack of thrombin signaling in platelets. *Journal of thrombosis and haemostasis : JTH* 2(8):1429-1435.
45. Matsushita K*, et al.* (2005) Vascular endothelial growth factor regulation of Weibel-Palade-body exocytosis. *Blood* 105(1):207-214.
46. Nightingale TD*, et al.* (2018) Tuning the endothelial response: differential release of exocytic cargos from Weibel-Palade bodies. *Journal of thrombosis and haemostasis : JTH* 16(9):1873-1886.
47. Matsushita K, Morrell CN, & Lowenstein CJ (2004) Sphingosine 1-phosphate activates Weibel-Palade body exocytosis. *Proceedings of the National Academy of Sciences of the United States of America* 101(31):11483-11487.
48. Chieng-Yane P*, et al.* (2011) Protease-activated receptor-1 antagonist F 16618 reduces arterial restenosis by down-regulation of tumor necrosis factor alpha and matrix metalloproteinase 7 expression, migration, and proliferation of vascular smooth muscle cells. *The Journal of pharmacology and experimental therapeutics* 336(3):643-651.
49. Kuliopulos A*, et al.* (2020) PAR1 (Protease-Activated Receptor 1) Pepducin Therapy Targeting Myocardial Necrosis in Coronary Artery Disease and Acute Coronary Syndrome Patients Undergoing Cardiac Catheterization: A Randomized, Placebo-Controlled, Phase 2 Study. *Arteriosclerosis, thrombosis, and vascular biology* 40(12):2990-3003.

50. Ren D*, et al.* (2022) Activated Protein C Strengthens Cardiac Tolerance to Ischemic Insults in Aging. *Circulation research* 130(2):252-272.
51. Antoniak S*, et al.* (2018) Protease-activated receptor 1 activation enhances doxorubicin-induced cardiotoxicity. *J Mol Cell Cardiol* 122:80-87.
52. Mosnier LO, Zlokovic BV, & Griffin JH (2014) Cytoprotective-selective activated protein C therapy for ischaemic stroke. *Thrombosis and haemostasis* 112(5):883-892.
53. Antoniak S*, et al.* (2017) Protease-Activated Receptor 1 Enhances Poly I:C Induction of the Antiviral Response in Macrophages and Mice. *J Innate Immun* 9(2):181-192.
54. Boucher AA*, et al.* (2020) Cell type-specific mechanisms coupling protease-activated receptor-1 to infectious colitis pathogenesis. *Journal of thrombosis and haemostasis : JTH* 18(1):91-103.

Figure 1

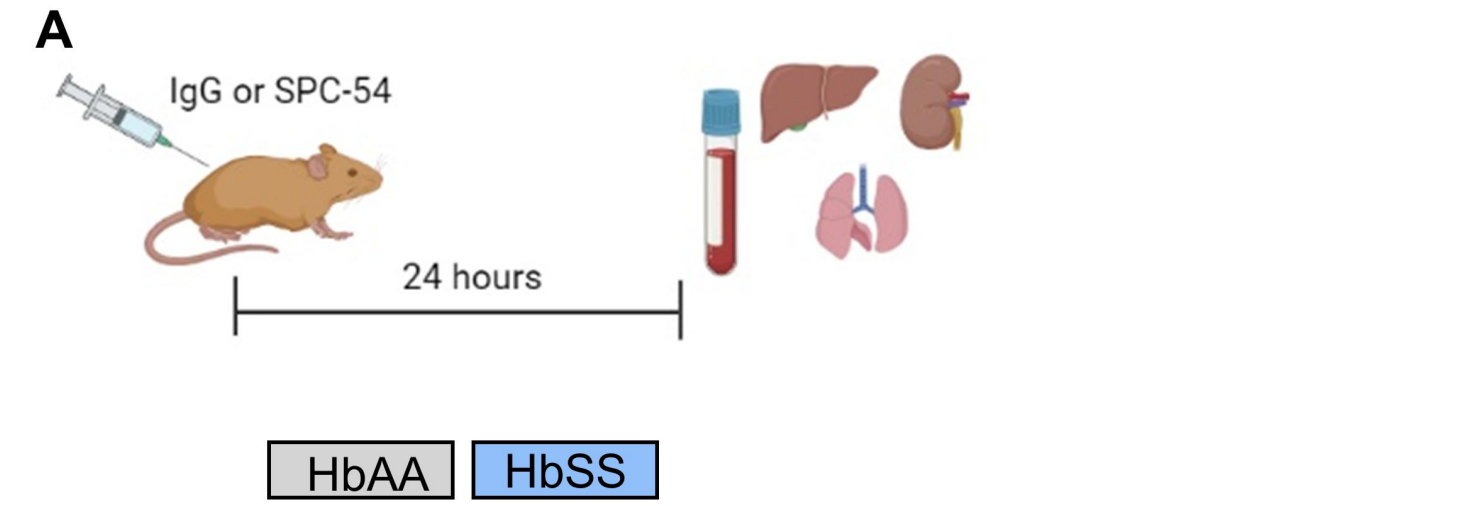

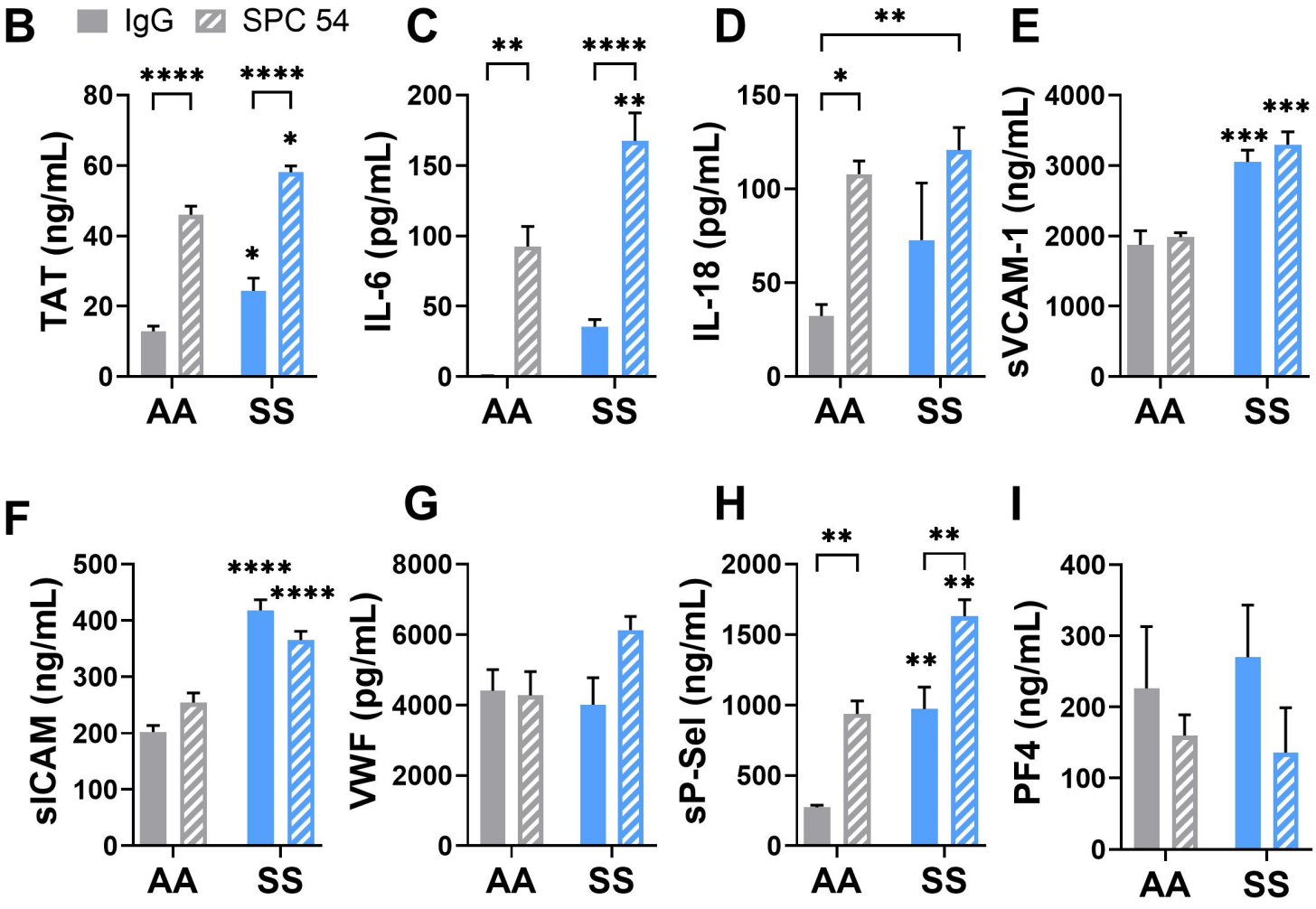

Figure 2

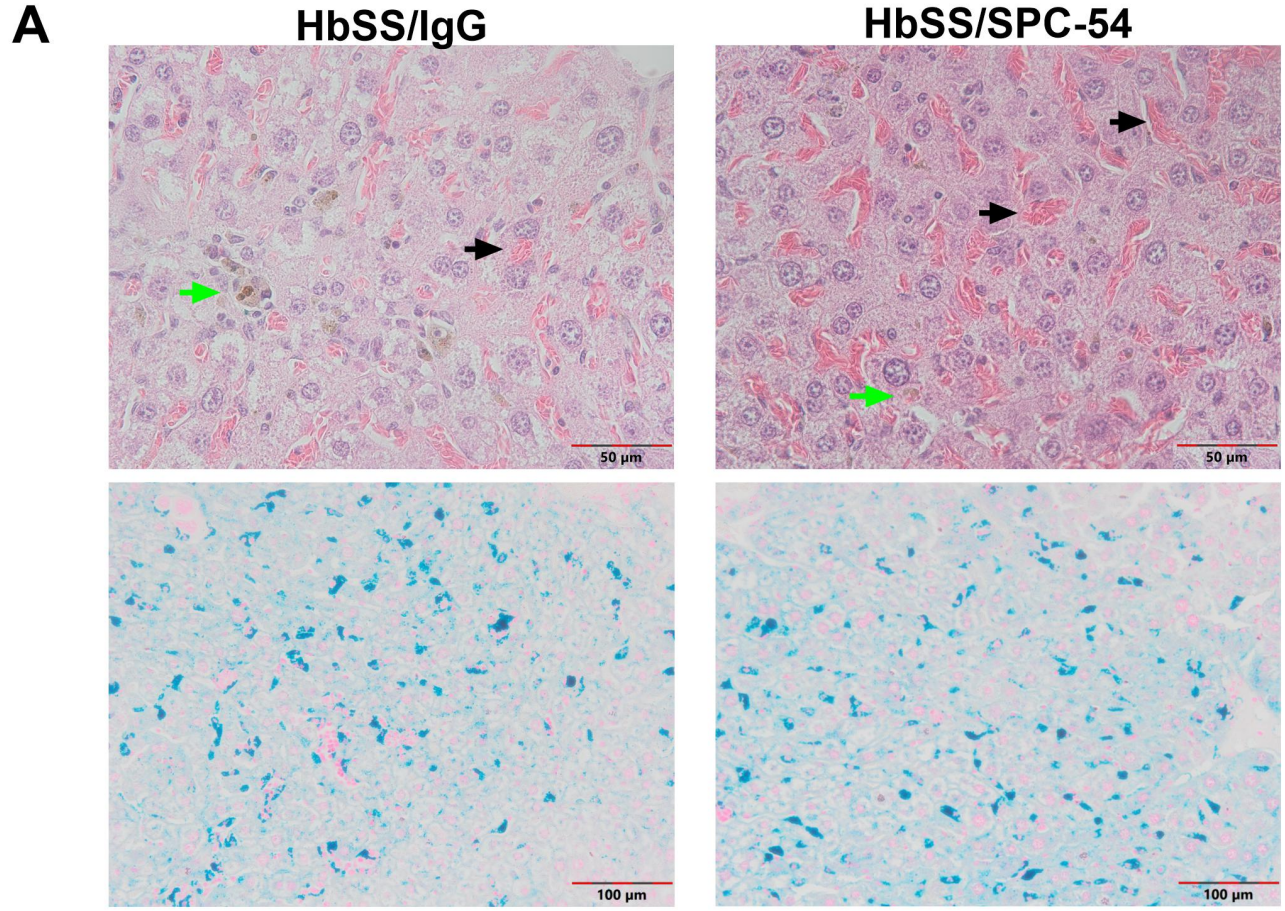

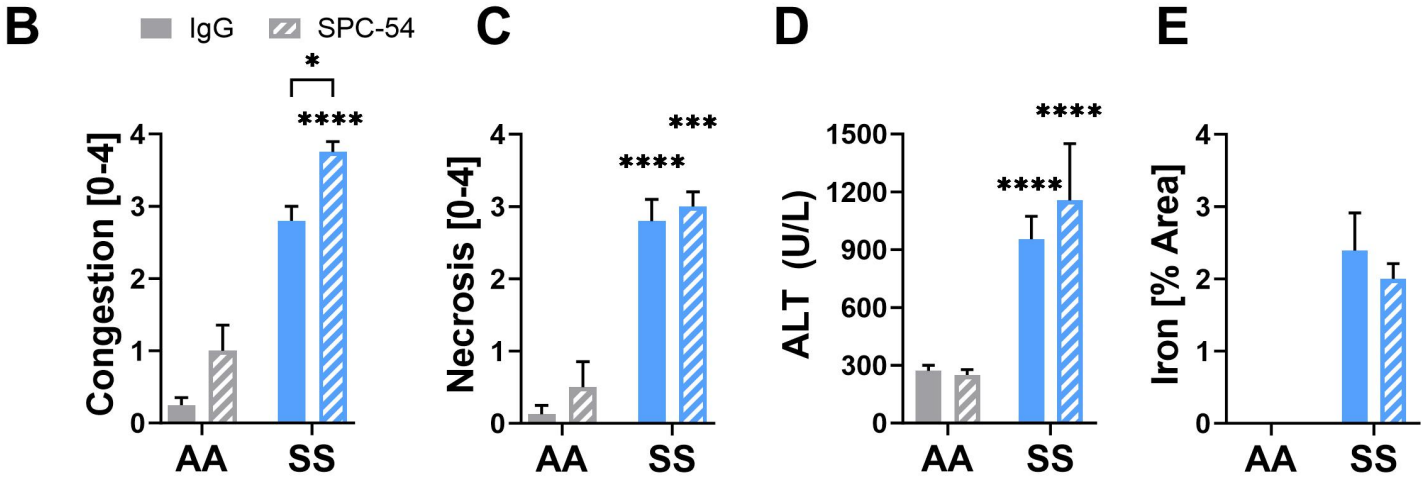

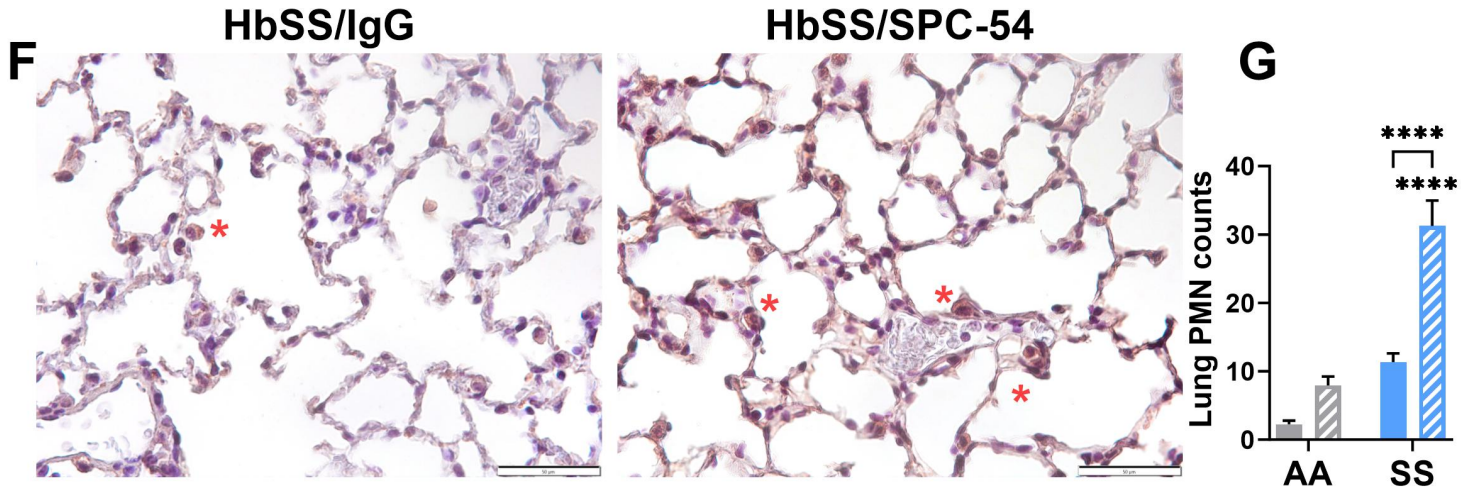

Figure 3

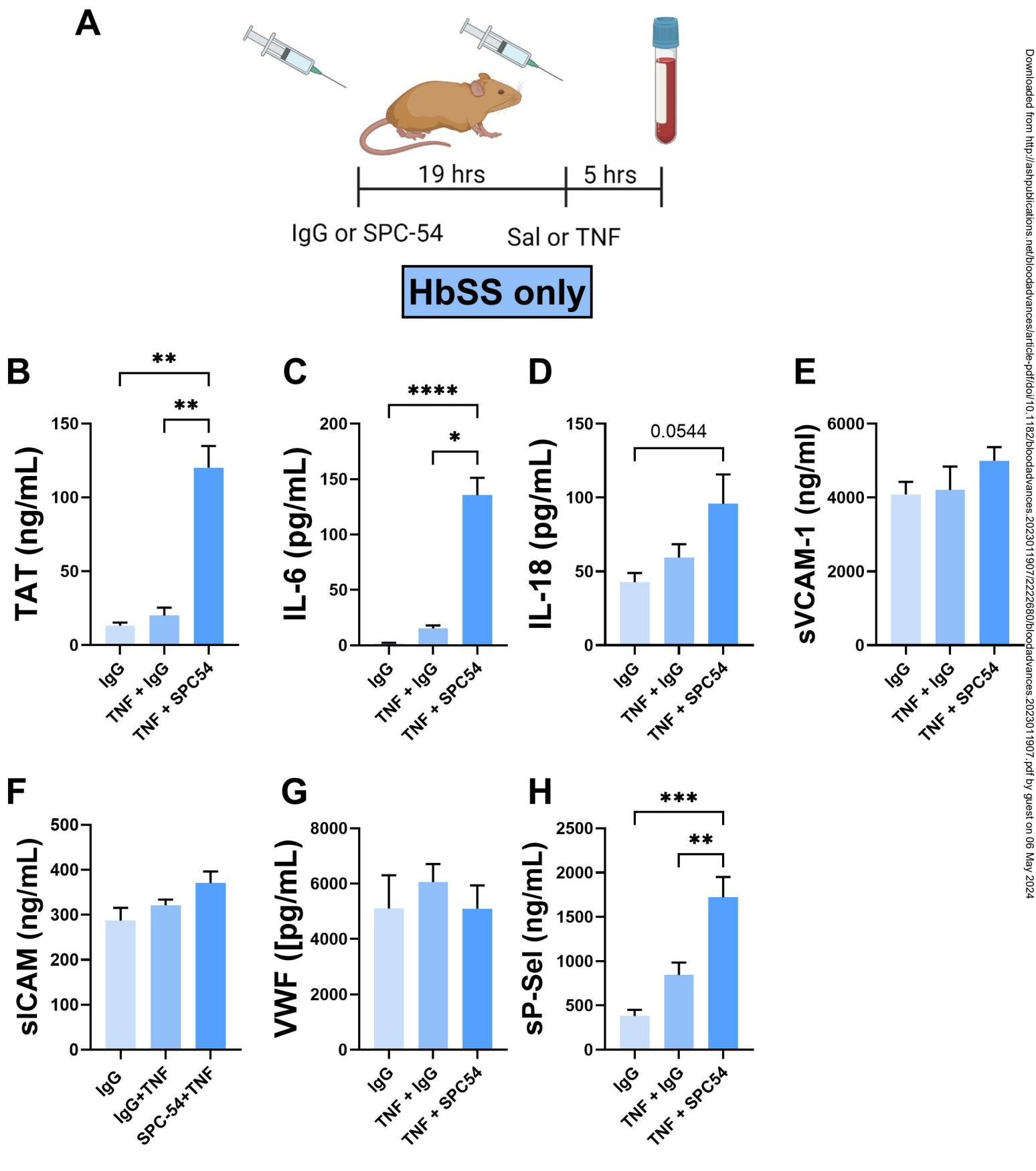

Figure 4

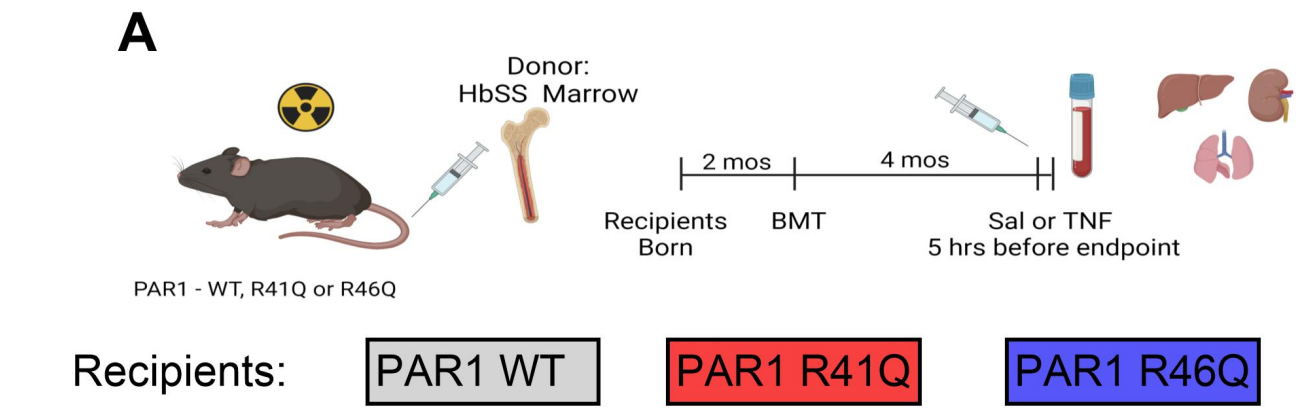

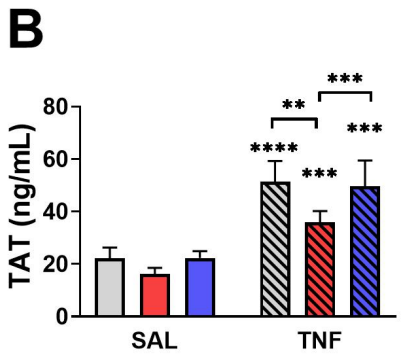

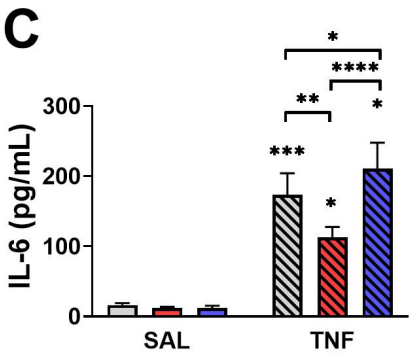

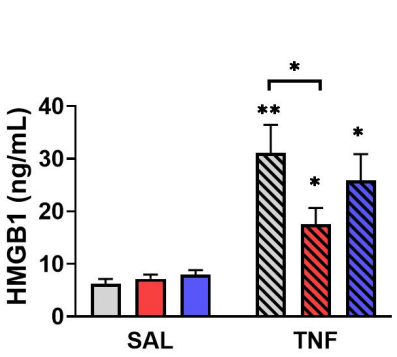

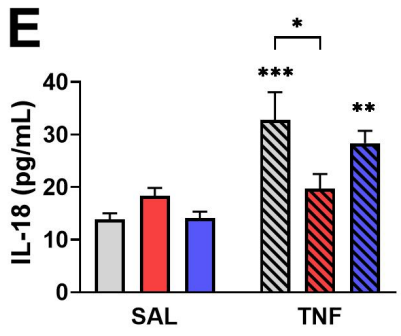

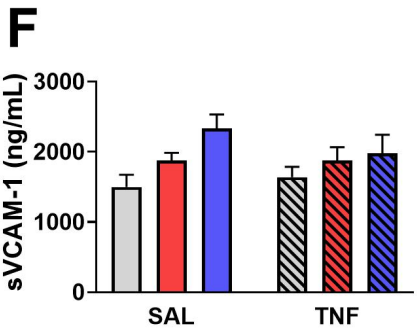

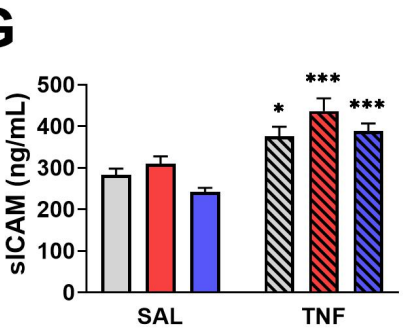

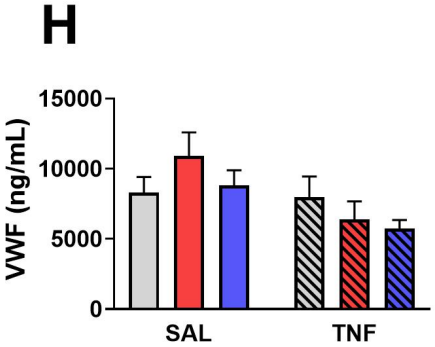

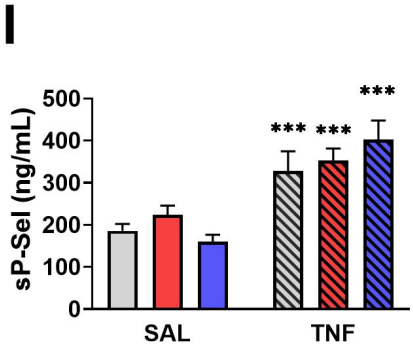

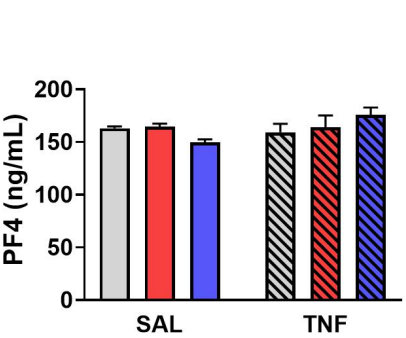

Figure 5